SINTERING OF TRANSIENT Al_2O_3 PHASES IN MONOLITHIC GELS

KATARÍNA BODIŠOVÁ, LADISLAV PACH, VLADIMÍR KOVÁR

Faculty of Chemical and Food Technology, Slovak University of Technology, Radlinského 9, 81237 Bratislava, Slovak Republic

E-mail: katarina.bodisova@stuba.sk

Submitted May 26, 2005; accepted July 7, 2005

Keywords: Boehmite gel, Sintering, Kinetics, Nanoparticles

The sintering of transient alumina phases in boehmite derived alumina gels was carried out under static thermal conditions (at sintering temperatures between 1075-1225°C) and under dynamic thermal conditions (in temperature range approximately 800-1200°C). At a low heating rate (2-10°C/min) the sintering of transient Al_2O_3 phases could be modeled by grain boundary and simultaneous bulk diffusion with activation energies 323 kJ/mol and 511 kJ/mol, respectively. At rapid heating the sintering kinetics is probably affected also by the remaining water escape. It can cause particle rearrangement in the first stage of sintering. Weight loss experiments were used to determine the amount of water escaped during sintering.

INTRODUCTION

Boehmite derived alumina gels are often used for preparing porous ceramics for catalysis and membrane processes [1]. The high volume change of gels at drying and sintering limits its utilization for bulk alumina ceramics except for abrasive grains [2].

Sintering kinetics helps to explain the sintering mechanism, which is useful for science as well as for technology. Kinetic analysis can be used under isothermal or non-isothermal conditions. In order to observe possible differences in the sintering mechanism at rapid heating it seems necessary to use both methods.

Despite the great importance of transient Al_2O_3 phases for the mentioned technologies, only little attention is paid to sintering kinetics of these phases, perhaps because of their transformations, which complicate the considerations about the sintering mechanism. Therefore the majority of authors focus on the sintering of α-Al_2O_3 powder compacts. They concluded that the material transport during sintering of fine-grained alumina at high temperature is rate-controlled by grain boundary diffusion [3, 4, 5].

Recently, nanosystems became a frequent object of study, especially the preparation of ceramics from nanopowders. Consequently great interest is paid to peptizable boehmite because it is easily available in nanoparticle form, in contrast to α-Al_2O_3 [6]. With respect to the particle size of the boehmite used, sintering of the Al_2O_3 gels can be classified as nanosintering [7]. This means that the involvement of another transport mechanism like particle displacement or rotation should be taken into account. In addition, a high level of chemically adsorbed gases can be assumed because of the high surface area of gels. In the case of boehmite the escape of water from remaining OH groups can be considered, too. As water and gases escape, the diffusivity of the system and the vacancy concentration can be changed. Thereby the sinterability of monoliths increases. Hence the escape of water or gases can be considered as one of the parameters influencing the sintering. The heating rate, especially at rapid heating, is another parameter discussed, the effect of which is significant primarily in nanosystems [7].

This study focuses on the sintering kinetics of transient Al_2O_3 phases (boehmite derived monolithic gels) under isothermal condition at rapid heating and uses also dilatometric measurement at constant heating rates. The water escape was observed at the same heat treatment as the sintering. The kinetic parameters of sintering were calculated using the equation derived by Johnson and Cutler [3] for different sintering mechanisms.

EXPERIMENTAL

Monolithic Al_2O_3 gels were prepared from commercial boehmite (Condea Pural, primary particle size ~5 nm) using the procedure described previously [8]. Water boehmite suspension was peptized by mixing with HNO_3 ($pH \cong 2.5$) at 55°C. The unpeptized part of the boehmite was eliminated from the sol by centrifugation (9000 rpm). The boehmite sol was poured into a plastic plate. A thin layer of sol was gelled in about 20 minutes. The gel was left to dry at room temperature for 3 days, which cracked spontaneously into large planar fragments (1-3 cm^2, thickness 2 mm). Monolithic gel fragments (~1 cm^2) were used for experiments. Planar gel samples were calcined at 550°C for 1 hour.

Netzsch 402E dilatometer was used to obtain the shrinkage data at constant heating rates. Three different heating rates, i.e. 2°C/min, 5°C/min, 10°C/min were used to increase the temperature from 25°C to 1200°C. The shrinkage, temperature and time were recorded. The samples used for dilatometric measurements were abraded to the shape of rectangular block with the longest dimension of ~1 cm.

The same samples were used for isothermal experiments. The samples were heated in a standard electric furnace. Isothermal sintering temperatures were reached by extremely high heating rates (370-410°C/min) introducing the samples rapidly into the preheated furnace. After 2 minutes the temperature of samples was constant. The heating rates were determined by Pt-PtRh10 thermocouple, the digital voltmeter output signal and time were registered by computer.

The monolithic Al_2O_3 gel samples were sintered at 1075, 1100, 1140, 1150, 1190, 1200 and 1225°C for 120-900 s. The density of each specimen was measured by the Archimedes method. The standard deviation of repeated measurements was 0.016 g/cm^3. The amount of water released during sintering was estimated by following the weight loss of the sintered samples at the same heat treatment as the sintering was carried out.

RESULTS AND DISCUSSION

Kinetic analysis of non-isothermal experiments

The experimental length-time dependencies for heating rates 2, 5 and 10°C/min are illustrated in figure 1. The marked temperature ranges terminate the presence of transient Al_2O_3 phases, of which the sintering kinetics was analyzed. The beginnings of the mentioned ranges were determined by calculations according to equations (1) and (4). The ends of the ranges were determined according to DTA curves as the temperatures at which the transformation of θ-Al_2O_3 to α- Al_2O_3 began. The further parts of sintering were beyond the interest of this work.

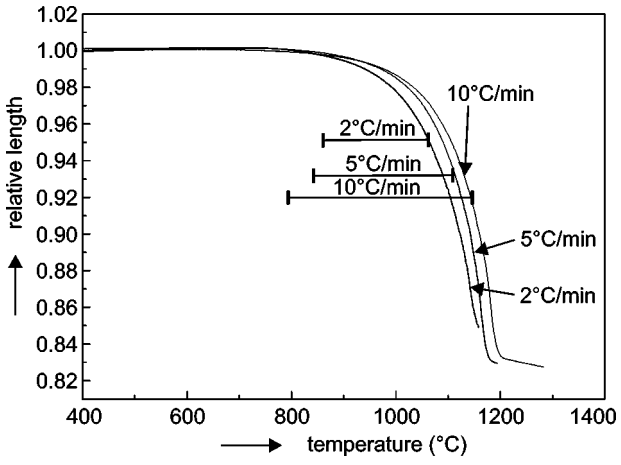

Figure 1. Experimental dependences of relative length on sintering time at heating rates 2, 5 and 10°C/min. The presence of transient alumina phases and hence the range of the kinetic analysis is designated by the segments.

In the mentioned ranges the bulk density increases from 1.522 to 1.891-2.028 g/cm^3. This represents an increase from 49.1 % to 54.5-57.1 % of the theoretical density, thus the densification corresponds to the initial state of sintering.

In the kinetic analysis of relevant parts of the curves in figure 1 (sintering of transient Al_2O_3 phases), we assumed at first that the sintering could be modeled by only one diffusive mechanism. Equation (1) [4] is in accordance with this assumption.

$$L_\tau = L_0\left\{1-\left[k\left(\tau-\tau_0\right)\right]^m\right\} \tag{1}$$

where L_τ is the actual sample length in time τ, L_0 the initial length, τ the experimental time, τ_0 the formal beginning of sintering, m a parameter independent on temperature (it is related to the sintering-controlled diffusion mechanism), k a kinetic constant, which is dependent on temperature according to Arrhenius equation (2)

$$k = A\exp\left(-\frac{E}{RT}\right) \tag{2}$$

where A is a preexponential factor, E the apparent activation energy, T the absolute temperature.

The correlation of the calculated and experimental values under the mentioned conditions was not acceptable for any dependence, probably because the model of one diffusive mechanism does not correspond to the reality of the process. Therefore the following calculation was curried out assuming two simultaneous densification mechanisms.

$$L_\tau = L_0\left\{1-\left[k_1\left(\tau-\tau_0\right)\right]^{m_1}-\left[k_2\left(\tau-\tau_0\right)\right]^{m_2}\right\} \tag{3}$$

The length - time dependencies were evaluated for each heating rate using equation (3) (the calculated parameters A_1, E_1, A_2, E_2, τ_0, m_1, m_2). The correlation of calculated and experimental values was suitable (0.99999), which supported the assumption of two diffusive mechanisms contributing to densification. Calculated parameters m_1 and m_2 were close to 0.31 and 0.46, respectively. Johnson et al. [4] presented the same values with physical meaning of grain boundary diffusion for the initial contact of two spheres (0.31) and bulk diffusion (0.46). Therefore we fixed these parameters and denoted them as m_g (= 0.31) and m_b (= 0.46) for subsequent calculations, so the equation (3) took form

$$L_\tau = L_0\left\{1-\left[k_g\left(\tau-\tau_{0,i}\right)\right]^{m_g}-\left[k_b\left(\tau-\tau_{0,i}\right)\right]^{m_b}\right\} \tag{4}$$

where subscript g denoted grain boundary diffusion, subscript b bulk diffusion and subscript i data file with appropriate heating rate.

The comparison of calculated parameters A and E showed that they were identical in all three cases. Therefore all three data files were evaluated together, assuming the validity of equation (4). The obtained results are presented in table 1 and in figure 2. The correlation of experimental and calculated values is very good (0.99998).

The calculation proved that the densification of boehmite derived Al_2O_3 monolithic gels could be modeled by grain boundary and simultaneous bulk diffusion. The densification of the monoliths begins approximately at 850°C with a significant contribution of grain boundary diffusion (figure 3). As the temperature increases the contribution of bulk diffusion rises and at about 1050°C the contribution of both mechanisms is approximately equal. Above this temperature the bulk diffusion becomes dominant.

According to many authors [8-11] α-Al_2O_3 sintering is controlled by the grain boundary diffusion with the apparent activation energy 415-620 kJ/mol. The apparent activation energy resulting from our evaluation for this process (323 kJ/mol) is rather lower probably because of another Al_2O_3 modification. Moreover, according to the used model, the bulk diffusion with the apparent activation energy 511 kJ/mol contributes significantly to the sintering, particularly above 1000°C.

The formal beginning of sintering depends on the heating rate; in our calculations it moves to slightly lower temperatures at higher rates, which could be considered as an unusual result. This apparent paradox agrees with Johnson's observations [13], which demonstrate that the high heating rates minimize the effects of the surface diffusion processes. Although these processes start earlier at the lower heating rates (comparing to the higher ones), they are not visible during dilatometric measurements, because the surface diffusion does not contribute to the densification of the compact body. Moreover, the surface diffusion processes decrease the sintering driving forces, so the beginning of the sintering moves to the higher temperatures.

On the contrary, at the higher heating rates, when a contribution of surface diffusion to total mass transport is lower, the driving force remains almost the same. The compact body then reaches higher temperatures in a highly sinterable state, the densification runs faster and it could therefore start at a lower temperature (comparing to the lower heating rates).

The sintering processes are likely influenced also by the gradual escape of water originating from the remaining OH groups (~2 wt.%). The amount of water released at the heating differs depending on the heating rate within the temperature range in which the sintering

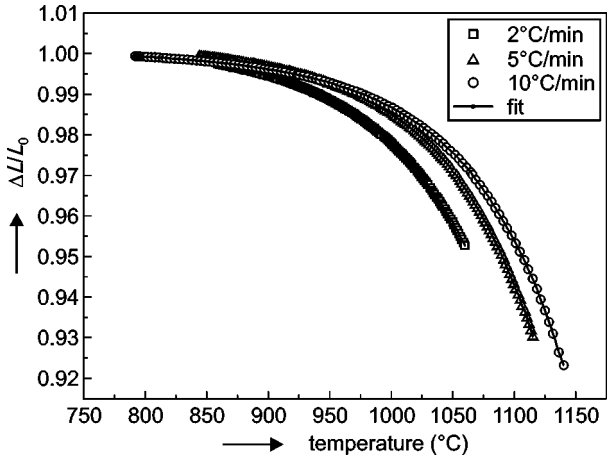

Figure 2. Relevant parts of experimental and calculated dependences of relative length on sintering time at heating rates 2, 5 a 10°C/min.

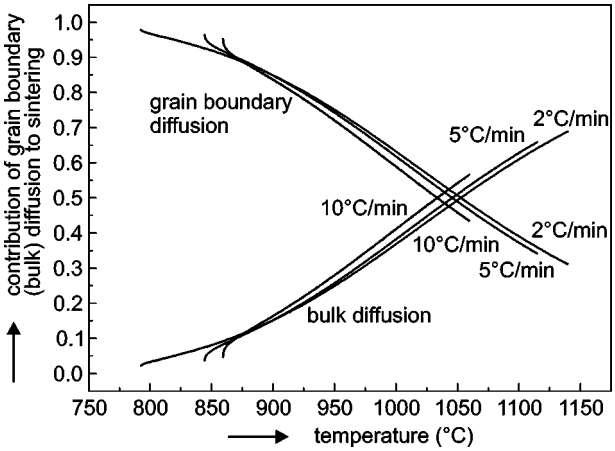

Figure 3. The contribution of several diffusion mechanisms to sintering in dependence on temperature at different heating rate.

Table 1. Parameters of equation (4) for non-isothermal sintering of transient alumina phases at different heating rates.

	Grain boundary diffusion		Bulk diffusion
A (s^{-1})	$2.4\times10^3 \pm 1.5\times10^3$		$6.1\times10^{12} \pm 2.7\times10^{12}$
E (kJ/mol)	323 ± 6		511 ± 5
m (fixed)	0.31		0.46
τ_0 (s) 2°C/min		10905 ± 30; 859 ± 1°C	
τ_0 (s) 5°C/min		5699 ± 12; 844 ± 1°C	
τ_0 (s) 10°C/min		4192 ± 6; 791 ± 1°C	

begins (figure 4). At faster heating, the monolith contains more water escaping with a significantly higher average rate (table 2) therefore its effect should be greater. At a higher heating rate the sintering begins at the lower temperature, hence we can conclude that the escape of water accelerates the sintering processes.

Kinetic analysis of isothermal experiments

Isothermal sintering was evaluated following experimental density - time dependencies at different sintering temperatures (1075, 1100, 1125, 1140, 1150, 1190, 1200 a 1225°C) at rapid heating (figure 5). The values in the range marked by dots were used in the analysis of sintering kinetics. In this range the isothermal sintering of transient Al_2O_3 phases takes place.

Table 2. The rate of water release at different heating rate.

Heating rate (°C/min)	Rate of water escape between 750-1000°C (referred to sample weight 1g) (g/min)
2	0.7×10^{-4}
10	2.5×10^{-4}

Table 3. Calculated parameters of equation (5) for isothermal sintering at temperatures 1140, 1150, 1190, 1200 a 1225°C.

	Grain boundary diffusion	Bulk diffusion
A (s^{-1})	$2.6\times10^{4} \pm 1.7\times10^{4}$	$9.6\times10^{13} \pm 1.0\times10^{13}$
E (kJ/mol) (fixed)	323	511
m (fixed)	0.31	0.46
τ_0 (s) 1140°C	95 ± 6	
τ_0 (s) 1150°C	92 ± 5	
τ_0 (s) 1190°C	88 ± 3	
τ_0 (s) 1200°C	84 ± 2	
τ_0 (s) 1225°C	82 ± 2	

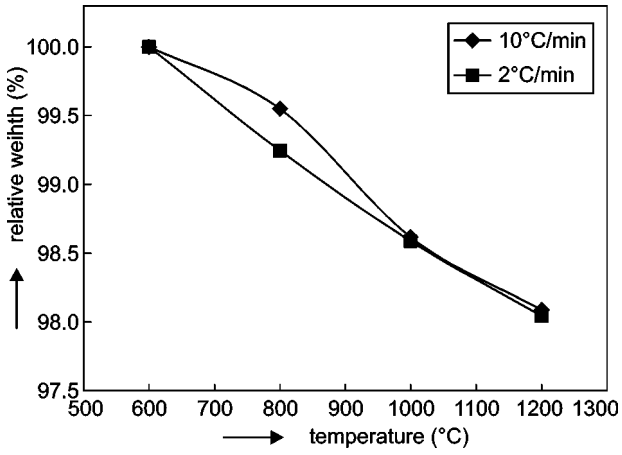

Figure 4. Weight loss of samples (due to escape of water) in dependence on temperature at different heating rate.

On the left side of this range there is a rapid temperature increase and on the right side the samples contain α-Al_2O_3 phase, so they are not in the scope of this work. The right border of this range was determined by X-ray analysis.

The sintering kinetics was evaluated in the same way as in the case of non-isothermal sintering assuming the simultaneous grain boundary and bulk diffusion mechanisms (m_g = 0.31, respective. m_b = 0.46) with effective activation energies E_g = 323 kJ/mol and E_b = 511 kJ/mol. For the case of bulk density dependence on time, the equation (4) can be transformed to the form

$$\rho_\tau = \frac{\rho_0}{\left\{1-\left[k_g\left(\tau-\tau_0\right)\right]^{m_g}-\left[k_b\left(\tau-\tau_0\right)\right]^{m_b}\right\}^3} \qquad (5)$$

where ρ_τ is the actual bulk density in time τ, ρ_0 - the bulk density at the beginning of sintering (for all dependencies the value is 1.522 g/cm^3, measured at room temperature); then the value τ_0 represents the formal beginning of sintering.

The results of calculations according to this equation were unsatisfactory. On the other hand the same results show that the proposed equation fits the experimental data for temperatures 1140-1225°C very well. Therefore the calculation was repeated only for the mentioned data sets. The results of this calculation are presented in table 3 and plotted in figure 6. (correlation = 0.998). Logically, the value of formal beginning of sintering decreases gradually with increasing temperature because at a higher temperature a shorter time is needed for reaching the temperature at which sintering begins. The contribution of bulk diffusion to densification is higher than 65 % and rises in dependence on the isothermal temperature up to 83 % for 1225°C (figure 7).

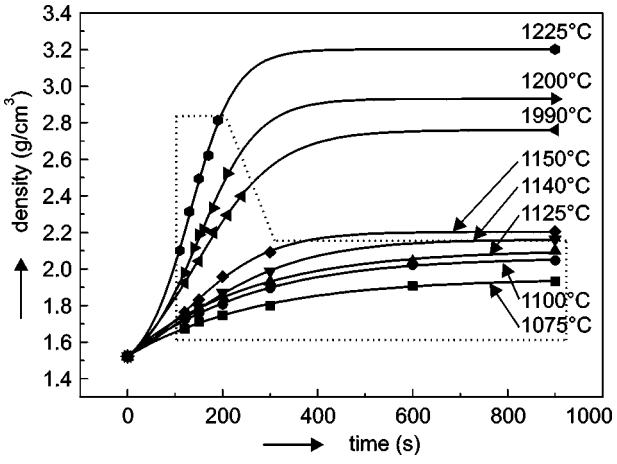

Figure 5. Experimental relative density - time dependences at sintering temperatures 1075, 1110, 1125, 1140, 1150, 1190, 1200 and 1225°C.

The data for sintering temperatures 1075, 1100 and 1125°C were evaluated by a similar equation.

$$\rho_\tau = \frac{\rho_0}{\left\{1-\left[k_1(\tau-\tau_0)\right]^{m_1}-\left[k_2(\tau-\tau_0)\right]^{m_2}\right\}^3} \quad (6)$$

The value of the parameter k_2 was close to zero and the value of m_1 was very close to the value 0.25, to which Johnson [4] assigned grain boundary diffusion for the initial contact plane - cone. Therefore these data were evaluated again using the equation

$$\rho_\tau = \frac{\rho_0}{\left\{1-\left[k(\tau-\tau_0)\right]^{0.25}\right\}^3} \quad (7)$$

The results are presented in table 4 and plotted in figure 8. For comparison, there are also calculated dependences using equation (5) in figure 8. It can be clearly seen that the model of two parallel diffusion mechanism does not fit the experimental values.

To explain the role of water escape from remaining OH groups the weight loss was observed under the same conditions as the sintering was carried out. The results are in table 5 and plotted in figure 9. The highest water escape (~75 %) occurs in the first 120 s, which is the heating period. This range is overlapped by range of the most intensive densification (the first 5 min). Relative high amount of water released in a short time (2 wt.% of water represent molar ratio $H_2O:Al_2O_3$ = 1 : 8.7) definitely influences the microstructure of monolith (possible particle rearrangement and cracks formation) the properties of sintered material and probably also the sintering mechanism.

Table 4. Parameters of equation (7) for isothermal shrinkage at temperatures 1075, 1100 and 1125°C.

A (s^{-1})	$2.3\times10^5 \pm 8.7\times10^5$
E (kJ/mol)	325 ± 44
m (fixed)	0.25
τ_0 (s) 1075°C	107 ± 7
τ_0 (s) 1100°C	103 ± 3
τ_0 (s) 1125°C	98 ± 8

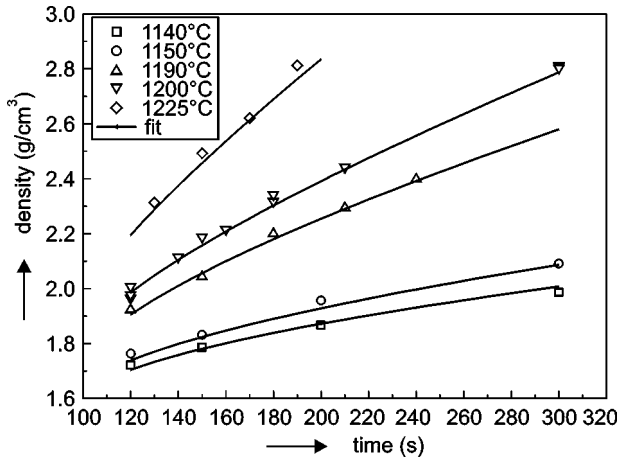

Figure 6. Relevant parts of experimental and calculated relative density - time dependences at sintering temperatures 1140, 1150, 1190, 1200 and 1225°C.

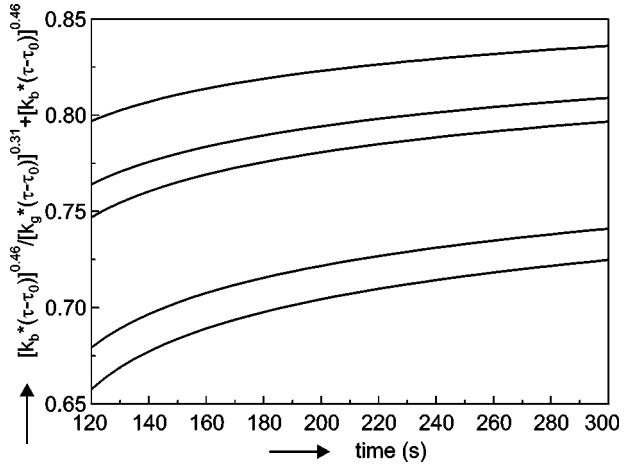

Figure 7. Contribution of bulk diffusion to densification at different isothermal temperatures.

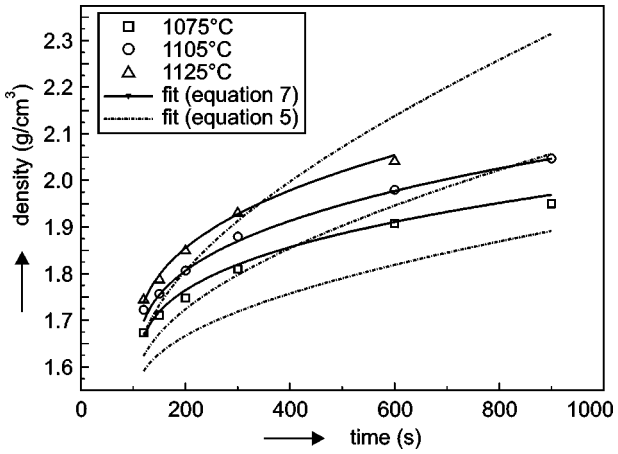

Figure 8. Experimental and calculated dependences of bulk density on time at sintering temperatures of 1075, 1100 and 1125°C.

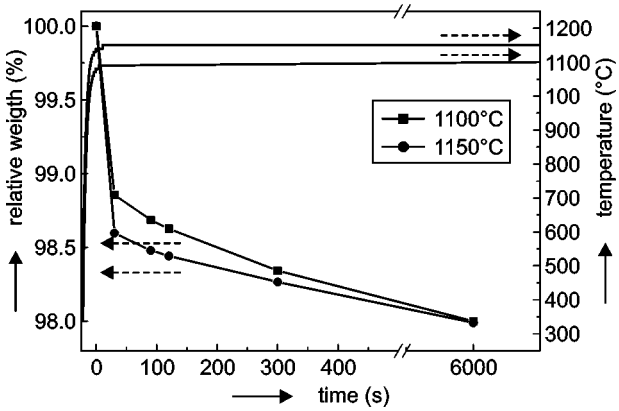

Figure 9. Relative weight of samples in dependence on time at different sintering temperatures.

Table 5. The rate of water release at different sintering temperatures.

Sintering temperature (°C)	Average rate of water escape (referred to sample weight 1g) (g/min)		
	up to 30 s	between 30 and 120 s	between 120 and 300 s
1100	2.3×10^{-2}	1.5×10^{-3}	9.4×10^{-4}
1150	2.8×10^{-2}	1.0×10^{-3}	5.9×10^{-4}

CONCLUSIONS

The kinetic parameters of transient Al_2O_3 sintering were evaluated following isothermal and non-isothermal measurements. The applied kinetic model supposes two diffusive mechanisms contributing to densification, namely grain boundary and bulk diffusion. The proposed equation fits the experimental data for non-isothermal sintering and for isothermal sintering at temperatures 1140-1225°C very well. Estimated apparent activation energies were for the both analysis 511 kJ/mol for bulk diffusion and 323 kJ/mol for grain boundary diffusion, respectively. These values are close to that published for α-Al_2O_3 sintering.

Experimental data for isothermal sintering at temperatures 1075, 1100 and 1125°C were well fitted by a similar equation, based on the assumption of only one diffusion mechanism (grain boundary diffusion).

The weight loss experiments sustain that ~2 wt.% of water escape during sintering of the gels. At slow heating, the molecules of water escape slowly thereby influence the densification mechanism only slightly, of course in dependence on heating rate. As a result, at enhanced heating rate the beginning of sintering is shifted to lower temperatures.

At rapid heating, a similar amount of water escapes up to 120 s, which most likely causes particle rearrangement in the monolith, so during the initial stage of sintering mass transport occurs not only by diffusive mechanisms. Particle rearrangement is influenced by water (gas) release.

Acknowledgement

The work has received financial support from the Slovak Grant for Science and Technology VEGA No 1/1380/04.

References

1. Li G., Smith Jr. R. L., Inomata H., Arai K.: Mater.Lett. *53*, 175 (2002).
2. Bača L., Pach L., Hrabě Z.: Ceramics-Silikáty *43*, 12 (1999).
3. Johnson D. L., Cutler I. B.: J.Am.Ceram.Soc. *46*, 541 (1963).
4. Li J. G., Sun X.: Acta Mater. *48*, 3103 (2000).
5. Lim L. C., Wong P. M., Jan M.: Acta mater. *48*, 2263 (2000).
6. Sharma P. K., Varadan V. V., Varadan V. K.: J.Eur. Ceram.Soc. *23*, 659 (2003).
7. Groza J. R.: Nanostruct.Mater. *12*, 987 (1999).
8. Pach L., Rustum R., Komarneni S.: J.Mater.Res. *5*, 278 (1989).
9. Watanabe S., Yoshida H., Sakuma T.: Key Eng.Mater. *247*, 67 (2003).
10. Sao J. H., Harmer M. P.: Philos.Mag.Lett. *63*, 7 (1991).
11. Brosnan K. H., Messing G. L., Agrawal D. K.: J.Am. Ceram.Soc. *86*, 1307 (2003).
12. Johnson D. L. in: *Materials Science Research Vol. 16*, pp. 243 - 252, C. C. Kuczynski, A. E. Miller, G. A. Sargent (Eds.), Plenum Press, New York 1983.

SPEKANIE PRECHODNÝCH FÁZ Al_2O_3 V MONOLITICKÝCH GÉLOCH

KATARÍNA BODIŠOVÁ, LADISLAV PACH, VLADIMÍR KOVÁR

Fakulta chemickej a potravinárskej technológie, Slovenská technická univerzita, Radlinského 9, 812 37 Bratislava, Slovensko

Spekanie prechodných fáz oxidu hlinitého v géloch Al_2O_3 pripravených z böhmitu sa sledovalo za neizotermických podmienok pri konštantných rýchlostiach ohrevu (2, 5 a 10°C/min) v teplotnom intervale približne 800-1200°C a za izotermických podmienok pri šokovom ohreve a teplotách 1075-1225°C. Pri nízkych rýchlostiach ohrevu možno spekanie prechodných fáz Al_2O_3 modelovať difúziou po hraniciach zŕn a paralelnou objemovou difúziou, s aktivačnými energiami 323 kJ/mol a 511 kJ/mol. Rovnaký model vyhovuje aj izotermickému spekaniu pri teplotách 1140-1225°C. Pri spekaní gélov Al_2O_3 dochádza k úniku vody (~2 hm.%) pochádzajúcej zo zvyškových OH skupín. Pri pomalých rýchlostiach ohrevu sa voda uvoľuje pomaly, jej vplyv na spekanie je teda mierny. Pri šokovom ohreve je rýchlosť úniku tejto vody výrazne vyššia, čo môže spôsobovať reorganizáciu častíc v počiatočnom štádiu spekania.